

Beyond the thin-wall approximation : precise numerical computation of prefactors in false vacuum decay

Gerald V. Dunne*

Department of Physics, University of Connecticut, Storrs, CT 06269, USA

Hyunsoo Min[†]

Department of Physics, University of Seoul, Seoul 130-743, Korea

Abstract

We present a general numerical method for computing precisely the false vacuum decay rate, including the prefactor due to quantum fluctuations about the classical bounce solution, in a self-interacting scalar field theory modeling the process of nucleation in four dimensional spacetime. This technique does not rely on the thin-wall approximation. The method is based on the Gelfand-Yaglom approach to determinants of differential operators, suitably extended to higher dimensions using angular momentum cutoff regularization. A related approach has been discussed recently by Baacke and Lavrelashvili, but we implement the regularization and renormalization in a different manner, and compare directly with analytic computations made in the thin-wall approximation. We also derive a simple new formula for the zero mode contribution to the fluctuation prefactor, expressed entirely in terms of the asymptotic behavior of the classical bounce solution.

*Electronic address: dunne@phys.uconn.edu

[†]Electronic address: hsmin@dirac.uos.ac.kr

I. INTRODUCTION

The phenomenon of nucleation drives first order phase transitions in many applications in physics, most notably in particle physics, condensed matter physics, quantum field theory and cosmology. The semiclassical analysis of the rate of such a nucleation process was pioneered by Langer [1], who identified a semiclassical saddle point solution that gives the dominant exponential contribution to the rate, with a prefactor to the exponential given by the quantum fluctuations about this classical solution. The nucleation rate is given by the quantum mechanical rate of decay of a metastable "false" vacuum, ϕ_- , into the "true" vacuum, ϕ_+ . Decay proceeds by the nucleation of expanding bubbles of true vacuum within the metastable false vacuum [1, 2, 3, 4, 5, 6, 7, 8]. This picture may also be extended to finite temperature field theory [9, 10]. Computing the semiclassical prefactor requires the computation of the determinant of the differential operator associated with quantum fluctuations about the classical solution. This is a technically difficult problem. Thus, it is not possible to compute the fluctuation prefactor analytically, and so various approximation techniques have been developed. The most widely-studied is the so-called "thin-wall" approximation, in which the bubble wall thickness is small compared to the bubble radius [3, 4, 6]. This provides an elegant physical picture of nucleation and in this limit certain parts of the decay rate computation may be done analytically. A limited amount is also known analytically concerning the expansion beyond the leading thin-wall limit, in two dimensions [6, 11, 12], three dimensions [13, 14], and four dimensions [15]. Other important approaches to metastable decay use direct lattice simulations [16], the average effective action [17], and phase shift techniques [18].

The point of this present paper is to reduce the calculation of the decay rate to a straightforward numerical computation, without relying on any such approximation or expansion. The starting point for our approach is an extremely elegant and simple method, due to Gelfand and Yaglom [19], for computing the determinant of a one-dimensional differential operator. This technique is ideal for numerical implementation. However, its naive generalization to higher dimensions is divergent [20]. This is because in higher dimensions renormalization is important, and so we must regulate and renormalize the determinant. We present an analytic method of doing this using an angular momentum cutoff, and apply it to the problem of false vacuum decay. (This method has previously been used to compute

the quark mass dependence of the fermion determinant for quarks in the presence of an instanton background [21].) A related approach to false vacuum decay, also based on the Gelfand-Yaglom formula, has been developed recently by Baacke and Lavrelashvili [22], and we comment in Section IV B on the similarities and differences between our approaches.

Consider the Euclidean classical action

$$S_{\text{cl}}[\phi] = \int d^4x \left(\frac{1}{2}(\partial_\mu \phi)^2 + U(\phi) \right) \quad , \quad (1.1)$$

where the potential $U(\phi)$ has two nondegenerate classical minima, $\phi_- < \phi_+$, with $U(\phi_-) > U(\phi_+)$. For quantitative computations, and comparison with previous work, we consider the standard quartic potential [2, 4, 11, 12], whose form is illustrated in Figure 1:

$$U(\phi) = \frac{\lambda}{8} (\phi^2 - a^2)^2 - \frac{\epsilon}{2a} (\phi - a) \quad . \quad (1.2)$$

The parameter ϵ represents a constant external source breaking the degeneracy of the double well potential. In four dimensional spacetime, the mass dimensions of the couplings are:

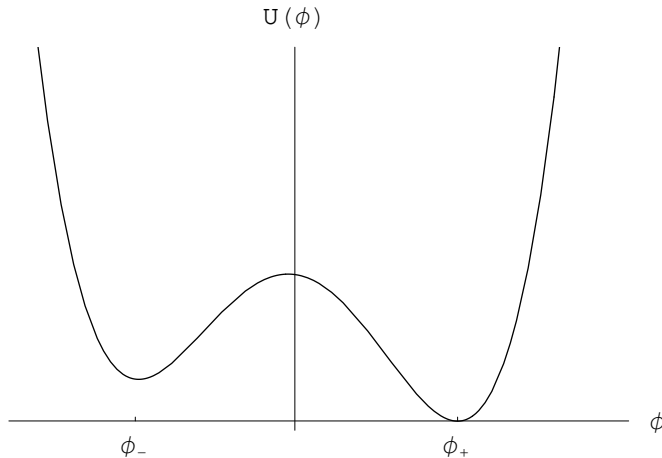


FIG. 1: Field potential $U(\phi)$ showing the true and false vacua, ϕ_+ and ϕ_- , respectively.

$[\lambda] = 0$, $[a] = 1$, and $[\epsilon] = 4$. We choose $a > 0$, $\lambda > 0$ and $\epsilon > 0$, in which case the two minima are $\phi_{\pm} = \pm a(1 \pm \frac{\epsilon}{2\lambda a^4} + \dots)$. Note that

$$U(\phi_-) - U(\phi_+) = \epsilon \left[1 + O\left(\frac{\epsilon}{\lambda a^4}\right) \right] \quad , \quad (1.3)$$

so for $\epsilon \ll \lambda a^4$, we see that ϵ has the physical interpretation as the potential energy difference between the two classical vacua. This small ϵ limit is known as the “thin-wall” limit [4]

because in this case the bubbles of true vacuum within the false vacuum have thin walls compared to their radius.

Expanding the field ϕ about the false vacuum ϕ_-

$$\phi = \phi_- + \varphi \quad , \quad (1.4)$$

and keeping terms up to dimension four, we find the potential, which is often considered directly in the literature [22]

$$U(\varphi) = \frac{m^2}{2}\varphi^2 - \eta\varphi^3 + \frac{\lambda}{8}\varphi^4 \quad . \quad (1.5)$$

Here m^2 and η are related to the original couplings by

$$m^2 = \frac{\lambda}{2}(3\phi_-^2 - a^2) \quad ; \quad \eta = \frac{\lambda}{2}|\phi_-| \quad . \quad (1.6)$$

In order to describe semiclassical tunneling, it is useful to rescale the field φ and the space-time coordinates as

$$\bar{x} = mx \quad ; \quad \varphi = \frac{m^2}{2\eta}\Phi \quad (1.7)$$

Then the classical action in terms of these dimensionless quantities is :

$$S_{\text{cl}}[\Phi] = \left(\frac{m^2}{4\eta^2}\right) \int d^4\bar{x} \left[\frac{1}{2}(\bar{\partial}_\mu\Phi)^2 + \frac{1}{2}\Phi^2 - \frac{1}{2}\Phi^3 + \frac{\alpha}{8}\Phi^4 \right] \quad . \quad (1.8)$$

The overall factor is determined by the dimensionless parameter

$$\beta = \frac{m^2}{4\eta^2} = \frac{1}{\lambda} \left(1 - \frac{\epsilon}{2\lambda a^4} + \dots \right) \quad . \quad (1.9)$$

For our semiclassical tunneling analysis, we assume $\beta \gg 1$. The quartic coupling strength in (1.8) is determined by the dimensionless quantity

$$\alpha = \frac{\lambda m^2}{4\eta^2} = 1 - \frac{\epsilon}{2\lambda a^4} + \dots \quad , \quad (1.10)$$

which tends to 1 in the "thin-wall" limit where $\epsilon \rightarrow 0$. The dimensionless parameter α determines the shape of the potential, and its deviation from 1 is a measure of the vacuum energy difference relative to the barrier height. Figure 2 shows some plots, for various values of α , of the dimensionless potential

$$U(\Phi) = \frac{1}{2}\Phi^2 - \frac{1}{2}\Phi^3 + \frac{\alpha}{8}\Phi^4 \quad . \quad (1.11)$$

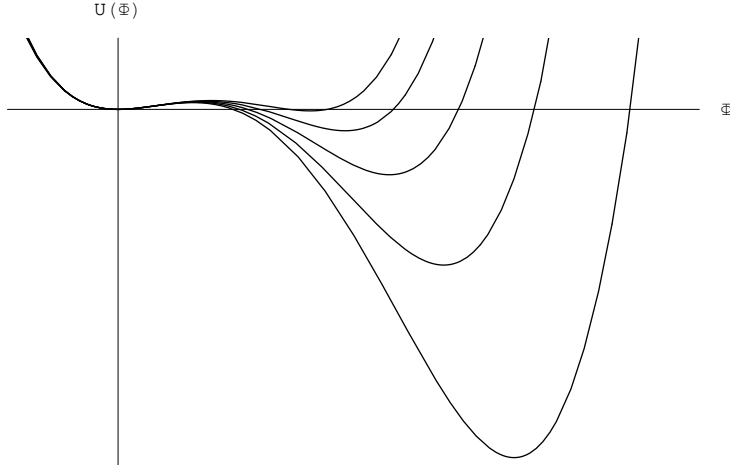


FIG. 2: Plots of the rescaled potential, $U(\Phi) = \frac{1}{2}\Phi^2 - \frac{1}{2}\Phi^3 + \frac{\alpha}{8}\Phi^4$, for $\alpha = 0.6, 0.7, 0.8, 0.9, 0.99$. As α approaches 1, the vacua become degenerate.

The false vacuum decay rate per unit volume and unit time is denoted γ , and its one-loop expression is [1, 2, 3, 4, 5, 6, 7, 8]

$$\gamma = \left(\frac{S_{\text{cl}}[\Phi_{\text{cl}}]}{2\pi} \right)^2 \left| \frac{\det'(-\square + U''(\Phi_{\text{cl}}))}{\det(-\square + U''(\Phi_-))} \right|^{-1/2} e^{-S_{\text{cl}}[\Phi_{\text{cl}}] - \delta_{\text{ct}}S[\Phi_{\text{cl}}]} \quad , \quad (1.12)$$

where the prime on the determinant means that the zero modes (corresponding to translational invariance) are removed. Here Φ_{cl} is a classical solution known as the “bounce” solution [4], defined below, and the prefactor terms in (1.12) correspond to quantum fluctuations about this bounce solution. The second term in the exponent, $\delta_{\text{ct}}S[\Phi_{\text{cl}}]$, denotes the counterterms needed for renormalization. The computational challenge is to evaluate the rate γ given a particular form of the classical potential. For our particular quartic model this corresponds to computing the rate for various values of β and α , the dimensionless parameters defined above in (1.9) and (1.10).

In the language of quantum field theory [3, 4, 7], γ is half the imaginary part of the generating functional of the connected Green’s functions with the constant external source, $-\frac{\epsilon}{2a}$, divided by the spacetime volume factor, and so we are essentially computing the renormalized effective action for this system [23, 24]. It is not possible to compute this tunneling rate γ analytically. Indeed, it is not even possible to find the classical bounce solution, Φ_{cl} , analytically, let alone the quantum fluctuations about this classical solution. We present here a simple numerical technique to compute γ for general forms of $U(\phi)$. This

technique involves a combination of an analytical computation and a numerical computation. The analytical part of the computation is related to the regularization and renormalization of the one loop effective action. The numerical part is elementary, and can be implemented straightforwardly and efficiently in Mathematica.

In Section II we describe how to compute the classical bounce solution numerically with very high precision. In Section III we describe how to compute the determinant prefactor arising from quantum fluctuations about the classical bounce solution. In Section IV we explain how to regularize and renormalize our answer using the angular momentum cutoff regularization and renormalization scheme developed previously in [21]. Our approach is related to an elegant technique presented recently by Baacke and Lavrelashvili [22], and in Section IV we also compare and contrast these two methods. In Section V we conclude with some general comments about possible further applications, and in the Appendix we present the derivation of a simple new formula for the contribution to the decay rate γ coming from the zero modes.

II. COMPUTING THE CLASSICAL BOUNCE SOLUTION

The first step in computing the false vacuum decay rate γ is to find the classical bounce solution, $\Phi_{\text{cl}}(r)$, which is an $0(4)$ -symmetric stationary point of the classical Euclidean action, with $\Phi_{\text{cl}}(r)$ interpolating between the false and true vacuum as r goes from 0 to ∞ [4, 25]. The action evaluated on the classical bounce solution determines the leading exponential factor in (1.12), and the quantum fluctuations about the classical bounce solution lead to the determinant prefactors in (1.12).

The bounce $\Phi_{\text{cl}}(r)$ solves the nonlinear ordinary differential equation

$$-\Phi_{\text{cl}}'' - \frac{3}{r}\Phi_{\text{cl}}' + \Phi_{\text{cl}} - \frac{3}{2}\Phi_{\text{cl}}^2 + \frac{\alpha}{2}\Phi_{\text{cl}}^3 = 0 \quad (2.1)$$

with boundary conditions

$$\Phi_{\text{cl}}'(0) = 0 \quad (2.2)$$

$$\Phi_{\text{cl}}(r) \rightarrow \Phi_- \equiv 0 \quad , \quad \text{as } r \rightarrow \infty \quad . \quad (2.3)$$

It is not known how to find $\Phi_{\text{cl}}(r)$ analytically in any nontrivial field theory. Much work has been done in the thin-wall approximation, which in practice means finding Φ_{cl} as an

expansion about the point $\alpha = 1$, where the two vacua are degenerate. The point of this present paper is to reduce the calculation of the tunneling rate γ to a straightforward numerical computation, without relying on any such approximation or expansion. Thus, we begin by determining $\Phi_{\text{cl}}(r)$ numerically.

To obtain extremely good precision we use a combination of both forward and backward shooting to compute $\Phi_{\text{cl}}(r)$. In forward shooting we numerically integrate (2.1) [using 4th order Runge-Kutta], starting at $r = 0$, and we adjust the initial value $\Phi_0 \equiv \Phi_{\text{cl}}(0)$ until the second boundary condition (2.3) is satisfied to a certain level of accuracy. Since one cannot start exactly at $r = 0$, we begin at some very small $r = r_0$ and use a Taylor expansion to write

$$\begin{aligned}\Phi_{\text{cl}}(r_0) &= \Phi_0 + \frac{1}{16}r_0^2 (2\Phi_0 - 3\Phi_0^2 + \alpha\Phi_0^3) \\ \Phi'_{\text{cl}}(r_0) &= \frac{1}{8}r_0 (2\Phi_0 - 3\Phi_0^2 + \alpha\Phi_0^3) \quad .\end{aligned}\tag{2.4}$$

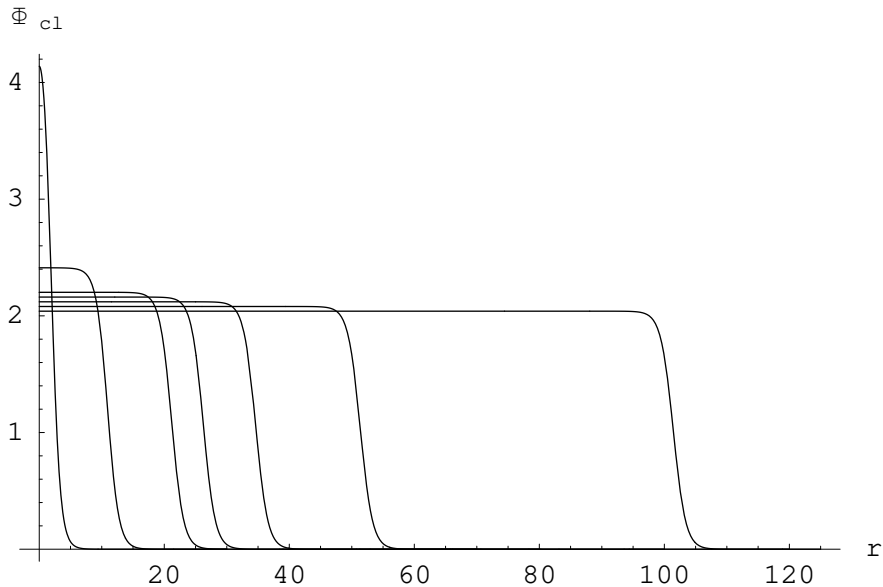


FIG. 3: Plots of the bounce solution $\Phi_{\text{cl}}(r)$ for various values of α : $\alpha = 0.5, 0.9, 0.95, 0.96, 0.97, 0.98, 0.99$, with the plateau ending farther to the right for increasing α . Observe that as $\alpha \rightarrow 1$, the sharp falloff in Φ_{cl} occurs at $r \sim \frac{1}{1-\alpha}$, and Φ_{cl} can be approximated by a step function.

We adjust the parameter Φ_0 until the large r boundary condition (2.3) is satisfied. In backward shooting we begin the numerical integration [also using 4th order Runge-Kutta]

at some very large $r = R$, with starting conditions

$$\Phi_{\text{cl}}(R) = \Phi_{\infty} \frac{K_1(R)}{R} \quad , \quad \Phi'_{\text{cl}}(R) = -\Phi_{\infty} \frac{K_2(R)}{R} \quad , \quad (2.5)$$

and adjust the parameter Φ_{∞} until the $r = 0$ boundary condition (2.2) is satisfied.

We first use forward shooting, which produces a good estimate of Φ_0 . Then using this bounce solution we estimate Φ_{∞} , and use this as a starting point for shooting backwards, which further refines this value of Φ_{∞} and also leads to a refined value of Φ_0 . It is a simple matter to obtain 20 - 30 decimal precision for each of Φ_{∞} and Φ_0 in this way. Some bounce profiles for various values of the coupling parameter α are shown in Figure 3.

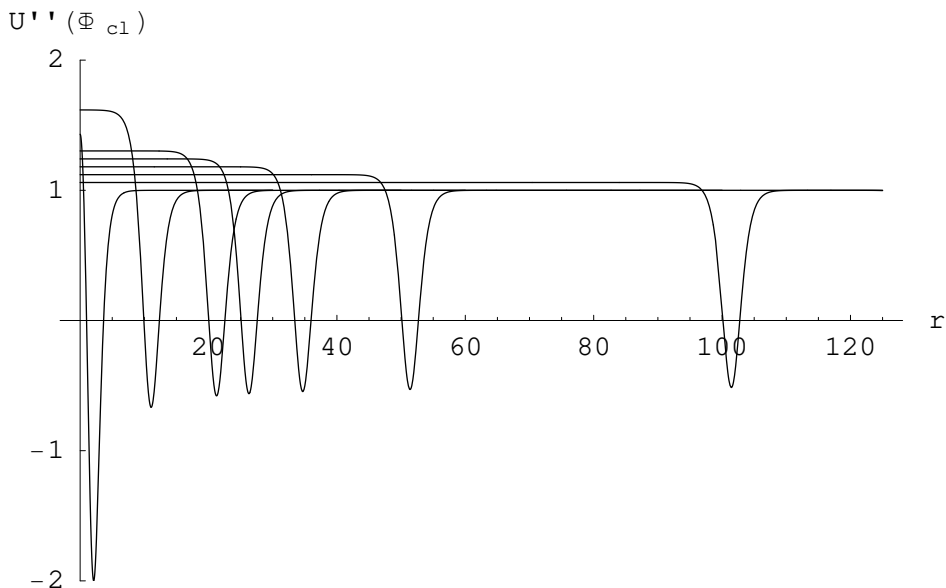


FIG. 4: Plots of the fluctuation potential $U''(\Phi_{\text{cl}}(r))$ for various values of α : $\alpha = 0.5, 0.9, 0.95, 0.96, 0.97, 0.98, 0.99$, with the binding well of the potential appearing farther to the right for increasing α . Observe that as $\alpha \rightarrow 1$, the potential $U''(\Phi_{\text{cl}}(r))$ is localized at $r \sim \frac{1}{1-\alpha}$, and is approximated well by the analytic form in (2.7).

Given the bounce solution, $\Phi_{\text{cl}}(r)$, the corresponding radial fluctuation potential is

$$U''(\Phi_{\text{cl}}(r)) = 1 - 3\Phi_{\text{cl}}(r) + \frac{3\alpha}{2}\Phi_{\text{cl}}^2(r) \quad . \quad (2.6)$$

Clearly, since $\Phi_{\text{cl}}(r)$ is only known numerically, the fluctuation potential $U''(\Phi_{\text{cl}}(r))$ is also only known numerically. Figure 4 shows some profiles of this fluctuation potential, corresponding to the various bounce profiles in Figure 3. Note that this fluctuation potential

is highly localized, with the localization radius depending strongly on α . As $\alpha \rightarrow 1$, the fluctuation potential binds states at radius $r \sim \frac{1}{1-\alpha}$, the radius of the bubble of false vacuum. Moreover, in this thin-wall limit, the minimum of the potential approaches $-1/2$, and outside the binding well it approaches 1. In fact, as noted in Langer's original work [1], in this limit $U''(\Phi_{\text{cl}}(r))$ is approximated well by the analytic potential

$$U''(\Phi_{\text{cl}}(r)) \sim 1 - \frac{3}{2} \operatorname{sech}^2 \left(\frac{1}{2} \left[r - \frac{1}{1-\alpha} \right] \right) . \quad (2.7)$$

III. COMPUTING THE DETERMINANT PREFACTOR

Since the bounce solution $\Phi_{\text{cl}}(r)$ is a function of r , the fluctuation operator $[-\square + U''(\Phi_{\text{cl}})]$ can be decomposed into partial waves, with (dimensionless) radial operators

$$\mathcal{M}_{(l)} = -\frac{d^2}{dr^2} - \frac{3}{r} \frac{d}{dr} + \frac{l(l+2)}{r^2} + 1 + V(r) , \quad (3.1)$$

of degeneracy $(l+1)^2$, with $l = 0, 1, 2, \dots$. Here the radial potential $V(r)$ is equal to the fluctuation potential (2.6) with its large radius asymptotic value, 1, subtracted:

$$V(r) = -3\Phi_{\text{cl}}(r) + \frac{3\alpha}{2}\Phi_{\text{cl}}^2(r) . \quad (3.2)$$

Likewise, the free fluctuation operator $[-\square + U''(\Phi_-)]$ can be decomposed into partial waves, with radial operators

$$\mathcal{M}_{(l)}^{\text{free}} = -\frac{d^2}{dr^2} - \frac{3}{r} \frac{d}{dr} + \frac{l(l+2)}{r^2} + 1 , \quad (3.3)$$

also of degeneracy $(l+1)^2$.

For each l , the ratio of the determinants of $\mathcal{M}_{(l)}$ and $\mathcal{M}_{(l)}^{\text{free}}$ can be computed efficiently and precisely using the Gelfand-Yaglom method [19, 20, 26, 27, 28, 29, 30]. This result states that for radial operators of the form (3.1,3.3),

$$\frac{\det(\mathcal{M}_{(l)})}{\det(\mathcal{M}_{(l)}^{\text{free}})} = \left(\lim_{R \rightarrow \infty} \left[\frac{\psi_{(l)}(R)}{\psi_{(l)}^{\text{free}}(R)} \right] \right)^{(l+1)^2} . \quad (3.4)$$

Here $\psi_{(l)}$ and $\psi_{(l)}^{\text{free}}$ are regular solutions of

$$\begin{aligned} \mathcal{M}_{(l)} \psi_{(l)} &= 0 \\ \mathcal{M}_{(l)}^{\text{free}} \psi_{(l)}^{\text{free}} &= 0 , \end{aligned} \quad (3.5)$$

with the *same* leading behavior at $r = 0$. By regularity we can choose this small r behavior to be

$$\begin{aligned}\psi_{(l)} &\sim r^l \quad , \quad r \rightarrow 0 \\ \psi_{(l)}^{\text{free}} &\sim r^l \quad , \quad r \rightarrow 0 \quad .\end{aligned}\tag{3.6}$$

This normalization choice fixes the free solution to be

$$\psi_{(l)}^{\text{free}}(r) = 2^{l+1}(l+1)! \frac{I_{l+1}(r)}{r}\tag{3.7}$$

where $I_{l+1}(r)$ is the modified Bessel function.

In fact, a numerical improvement comes from realizing that both $\psi_{(l)}(r)$ and $\psi_{(l)}^{\text{free}}(r)$ grow exponentially fast at large r , so it is numerically better to integrate directly the ratio [22]

$$T_{(l)}(r) \equiv \frac{\psi_{(l)}(r)}{\psi_{(l)}^{\text{free}}(r)} \quad ,\tag{3.8}$$

which satisfies the equation

$$T_{(l)}'' + \left(\frac{1}{r} + 2 \frac{I_{l+1}'(r)}{I_{l+1}(r)} \right) T_{(l)}' - V(r)T_{(l)} = 0 \quad ,\tag{3.9}$$

with simple *initial value boundary conditions*:

$$T_{(l)}(0) = 1 \quad ; \quad T_{(l)}'(0) = 0 \quad .\tag{3.10}$$

Then the result (3.4) is recast as

$$\frac{\det(\mathcal{M}_{(l)})}{\det(\mathcal{M}_{(l)}^{\text{free}})} = (T_{(l)}(\infty))^{(l+1)^2} \quad .\tag{3.11}$$

We stress that the result (3.11) provides a remarkably simple technique for computing the determinant of a radial differential operator. It does not require any detailed knowledge of the spectrum of the operator whose determinant is being computed, nor does it require evaluating and numerically integrating the associated phase shift. Furthermore, the result (3.11) is ideally suited to numerical evaluation, as initial value boundary conditions are straightforward to implement numerically.

There are three different types of eigenvalue of the fluctuation operator, each having a different role physically and mathematically.

- Negative Eigenvalue Mode : ($l = 0$)

The lowest eigenvalue mode in the $l = 0$ sector is a negative eigenvalue mode of the fluctuation operator, and is responsible for the instability leading to decay. It can be identified with homogeneous swelling and shrinking of the bubble of true vacuum. This mode contributes a factor to the decay rate γ related to the *absolute value* of the determinant of the $l = 0$ fluctuation operator [1, 4]. This determinant is computed by numerically integrating (3.9) for $l = 0$:

$$\left| \frac{\det \mathcal{M}_{(l=0)}}{\det \mathcal{M}_{(l=0)}^{\text{free}}} \right|^{-1/2} = |T_{(0)}(\infty)|^{-1/2} \quad . \quad (3.12)$$

- Zero Eigenvalue Modes : ($l = 1$)

In the $l = 1$ sector there is a four-fold degenerate zero eigenvalue of the fluctuation operator. Physically, these four zero modes are the Goldstone modes associated with the breaking of translational invariance. Integrating over the corresponding collective coordinates [31] produces the factors of $\frac{S_{\text{cl}}}{2\pi}$ in (1.12). In computing the rate γ , we need the determinant of the fluctuation operator with the zero modes removed [1, 4]. We have found the following simple new formula for the $l = 1$ sector prefactor contribution (see Appendix A for a derivation):

$$\left(\frac{S_{\text{cl}}[\varphi_{\text{cl}}]}{2\pi} \right)^2 \left(\frac{\det' \mathcal{M}_{(l=1)}}{\det \mathcal{M}_{(l=1)}^{\text{free}}} \right)^{-1/2} = \left[\frac{\pi}{2} \Phi_{\infty} \left(\Phi_0 - \frac{3}{2} \Phi_0^2 + \frac{\alpha}{2} \Phi_0^3 \right) \right]^2 \quad , \quad (3.13)$$

where $\Phi_0 = \Phi_{\text{cl}}(0)$ is the bounce solution evaluated at the origin, and Φ_{∞} is the coefficient of $K_1(r)/r$ in the large r behavior of $\Phi_{\text{cl}}(r)$, as in (2.5). The advantage of the result (3.13) is that it is expressed entirely in terms of the asymptotic behavior of the classical bounce solution $\Phi_{\text{cl}}(r)$. This asymptotic information is already generated in the precise numerical determination of the bounce solution, so no further computation is needed to extract the zero mode contribution to the prefactor.

- Positive Eigenvalue Modes : ($l \geq 2$)

For $l \geq 2$, the fluctuation operator has positive eigenvalues, each of degeneracy $(l+1)^2$. These modes correspond to deformations of the bubble shape and thickness. For each l , the associated radial determinant is computed simply by numerical integration of

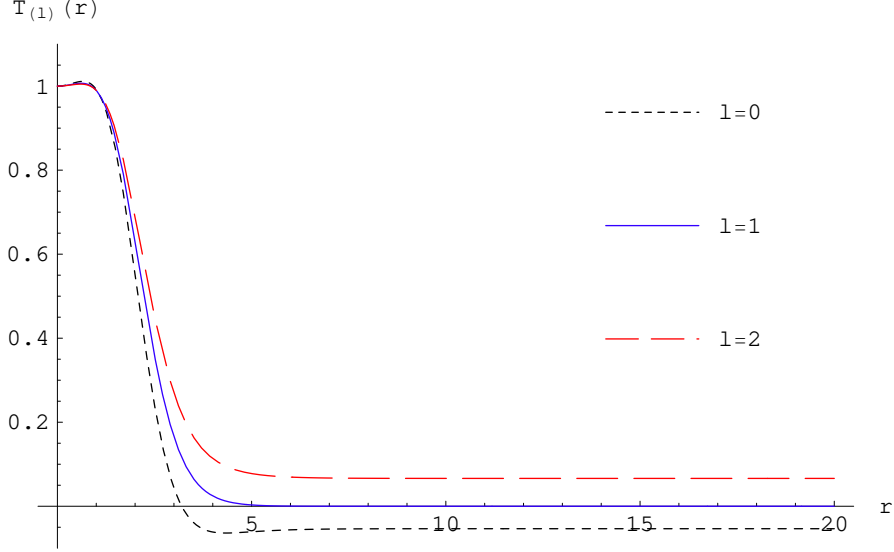


FIG. 5: Plots of $T_{(l)}(r)$ for $l = 0$, $l = 1$, and $l = 2$. These plots are for $\alpha = 0.5$. Note that the asymptotic value, $T_{(l)}(\infty)$, is negative for $l = 0$, zero for $l = 1$, and positive for $l = 2$, confirming the discussion in the text concerning the three different types of modes.

(3.9) with the initial value boundary conditions (3.10):

$$\left(\frac{\det \mathcal{M}_{(l)}}{\det \mathcal{M}_{(l)}^{\text{free}}} \right)^{-1/2} = [T_{(l)}(\infty)]^{-(l+1)^2/2} \quad . \quad (3.14)$$

Figure 5 shows plots of $T_{(l)}(r)$ as a function of r , for $l = 0$, $l = 1$, and $l = 2$. These plots are for $\alpha = 0.5$. Observe that $T_{(l)}(r)$ approaches very rapidly its asymptotic value, $T_{(l)}(\infty)$, for r outside the range of the binding well of the fluctuation potential (compare with Figure 4 for $\alpha = 0.5$). Also note that the asymptotic value, $T_{(l)}(\infty)$, is negative for $l = 0$, zero for $l = 1$, and positive for $l = 2$, confirming the discussion above of the three different types of modes.

For each partial wave with $l \geq 2$, the radial determinant, $[T_{(l)}(\infty)]^{(l+1)^2}$, is finite and simple to evaluate. In the discussion of renormalization it proves convenient to consider the *logarithm* of the determinant factors appearing in the rate (1.12):

$$-\frac{1}{2} \ln \left(\frac{\det \mathcal{M}_{(l)}}{\det \mathcal{M}_{(l)}^{\text{free}}} \right) = -\frac{1}{2} (l+1)^2 \ln T_{(l)}(\infty) \quad . \quad (3.15)$$

For large l we can use the radial WKB analysis of [21, 32] to find the leading behavior:

$$\ln T_{(l)}(\infty) \sim \frac{1}{(l+1)} \left[\frac{1}{2} \int_0^\infty dr r V(r) \right] + O \left(\frac{1}{(l+1)^3} \right) \quad . \quad (3.16)$$

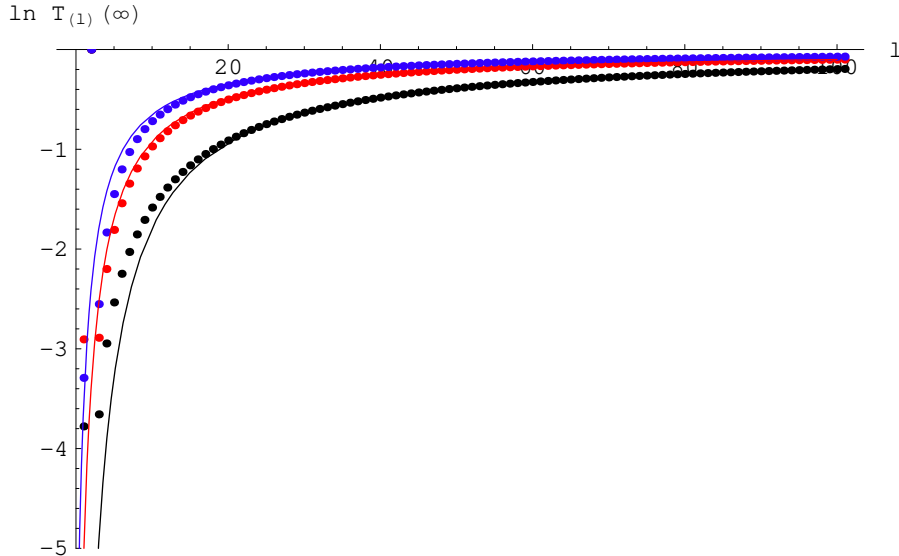


FIG. 6: The l dependence of $\ln T_{(l)}(\infty)$ for three different values of α : $\alpha = 0.01$ (top curve), $\alpha = 0.7$ (middle curve), and $\alpha = 0.9$ (bottom curve). The dots show the values of $\ln T_{(l)}(\infty)$ evaluated numerically using (3.9), while the solid lines show the WKB prediction (3.16) of the leading large l behavior. Notice the excellent agreement for $l \geq 20$.

The leading large l behavior (3.16) is illustrated in Figure 6 for several different values of the quartic coupling parameter α . Notice the very good agreement between the numerical results for $\ln T_{(l)}(\infty)$ [solid points] and the WKB estimate [curves from (3.16)]. Further subleading corrections to (3.16) are computed below in the next Section – see (4.14).

IV. REGULARIZATION AND RENORMALIZATION

The large l behavior (3.16) means that the formal sum of contributions (3.15) to $-\ln \gamma$,

$$\frac{1}{2} \sum_{l=2}^{\infty} (l+1)^2 \ln [T_{(l)}(\infty)] \quad , \quad (4.1)$$

is quadratically divergent. This divergence should not be too surprising, as we have neither regulated nor renormalized the determinant prefactor in the expression (1.12) for γ . In the language of quantum field theory, we need to compute the *renormalized* one-loop effective action for this interacting scalar field theory [3, 4, 6, 7]. Here we will apply the *angular momentum cutoff regularization and renormalization technique* developed in [21] which was successfully applied to the computation of the quark mass dependence of the fermion

determinant in an instanton background in QCD.

A. Regularization

The first step is to introduce a regulator mass μ using the proper-time representation of the logarithm :

$$\left[\ln \left(\frac{\det \mathcal{M}_{(l)}}{\det \mathcal{M}_{(l)}^{\text{free}}} \right) \right]_{\text{reg}} = -(l+1)^2 \int_0^\infty \frac{ds}{s} (\mu^2 s)^\varepsilon \text{tr} \left[e^{-s\mathcal{M}_{(l)}} - e^{-s\mathcal{M}_{(l)}^{\text{free}}} \right] \quad , \quad (4.2)$$

where the space-time dimension is extended to $4 - 2\varepsilon$, and we have explicitly extracted the degeneracy factor $(l+1)^2$ from the trace of the radial operators $\mathcal{M}_{(l)}$ and $\mathcal{M}_{(l)}^{\text{free}}$ defined in (3.1) and (3.3). We then split the sum over l of these regulated terms into two parts:

$$\begin{aligned} \frac{1}{2} \sum_{l=2}^{\infty} \left[\ln \left(\frac{\det \mathcal{M}_{(l)}}{\det \mathcal{M}_{(l)}^{\text{free}}} \right) \right]_{\text{reg}} &= \frac{1}{2} \sum_{l=0}^L \left[\ln \left(\frac{\det \mathcal{M}_{(l)}}{\det \mathcal{M}_{(l)}^{\text{free}}} \right) \right]_{\text{reg}} + \frac{1}{2} \sum_{l=L+1}^{\infty} \left[\ln \left(\frac{\det \mathcal{M}_{(l)}}{\det \mathcal{M}_{(l)}^{\text{free}}} \right) \right]_{\text{reg}} \\ &\equiv \Sigma_1 + \Sigma_2 \end{aligned} \quad (4.3)$$

Here L is a large but finite integer (in practice, we take L to be of the order of 50 to 100, depending on the value of α). Since Σ_1 is a finite sum we can safely remove the regulator μ and write

$$\Sigma_1 = \frac{1}{2} \ln |T_{(0)}(\infty)| - 2 \ln \left[\frac{\pi}{2} \Phi_\infty \left(\Phi_0 - \frac{3}{2} \Phi_0^2 + \frac{\alpha}{2} \Phi_0^3 \right) \right] + \frac{1}{2} \sum_{l=2}^L (l+1)^2 \ln T_{(l)}(\infty) \quad (4.4)$$

The first term in Σ_1 corresponds to the negative mode contribution (3.12), the second term is from the zero mode contribution (3.13), and the final sum corresponds to the contributions in partial waves with $2 \leq l \leq L$. Each term $T_{(l)}(\infty)$ in this last sum is evaluated numerically by solving (3.9). The second sum in (4.3)

$$\Sigma_2 \equiv -\frac{1}{2} \sum_{l=L+1}^{\infty} (l+1)^2 \int_0^\infty \frac{ds}{s} (\mu^2 s)^\varepsilon \text{tr} \left[e^{-s\mathcal{M}_{(l)}} - e^{-s\mathcal{M}_{(l)}^{\text{free}}} \right] \quad , \quad (4.5)$$

cannot be computed numerically using (3.9) because of the infinite sum and the presence of the regulator mass μ . Instead, we use radial WKB, which is a good approximation for large l , to compute *analytically* the leading large L behavior of Σ_2 . This is a straightforward

computation using the results of [21, 32]. The result is:

$$\begin{aligned} \Sigma_2 = \frac{1}{2} \left\{ -\frac{(L+1)(L+2)}{4} \int_0^\infty dr r V(r) + \frac{\ln L}{8} \int_0^\infty dr r^3 V(V+2) \right. \\ \left. - \frac{1}{16} \int_0^\infty dr \left(\frac{1}{\epsilon} + 2 - \gamma_E + \ln \frac{\mu^2 r^2}{4} \right) r^3 V(V+2) \right\} + 0 \left(\frac{1}{L} \right) . \end{aligned} \quad (4.6)$$

Here γ_E is Euler's constant. Note that this WKB computation reveals large L divergences going like L^2 , L and $\ln L$, in addition to a term which is finite in the large L limit. These last two terms are exactly of the form expected for renormalization, as is discussed in the next section.

The most important observation at this stage is that the large L divergences of Σ_2 cancel *exactly* the large L divergence found numerically in Σ_1 , leaving a finite answer. Indeed, comparing (4.6) with (3.16) we see immediately that the quadratic divergence cancels. Extending (3.16) to include 2nd order WKB contributions proves the cancellation of the sub-leading divergences also.

B. Renormalization

In standard perturbative renormalization theory, the self-interacting scalar field theory described by the action (1.1) involves two renormalization parameters, λ and a^2 , together with the wave function renormalization Z . The renormalization counter terms can be found by replacing those parameters with $\lambda + \delta\lambda$, and $a^2 + \delta a^2$. The one-loop approximations can be found in quantum field theory text books (see, *e.g.* [35]) :

$$\delta\lambda = \frac{9\lambda^2}{32\pi^2} \left(\frac{1}{\epsilon} - \gamma_E \right) \quad (4.7)$$

$$\delta(\lambda a^2) = \frac{3\lambda^2 a^2}{32\pi^2} \left(\frac{1}{\epsilon} - \gamma_E \right), \quad (4.8)$$

and $Z = 1$, in the $\overline{\text{MS}}$ renormalization scheme using dimensional regularization. With this replacement we identify the renormalization counterterms as

$$\delta_{ct} S = \int d^4x \left[\frac{\delta\lambda}{8} (\phi^2 - a^2)^2 - \frac{\lambda \delta a^2}{4} (\phi^2 - a^2) \right] \quad (4.9)$$

$$= \frac{1}{32} \int_0^\infty dr \left(\frac{1}{\epsilon} - \gamma_E \right) r^3 V(V+2). \quad (4.10)$$

In obtaining (4.10) from (4.9) we have used (1.4), (1.6), (1.7), (1.10), and (3.2) to translate from the original physical field ϕ , and couplings λ and a^2 , to the field Φ and coupling α

which correspond to expanding the field about the false vacuum ϕ_- . Notice the appearance in (4.10) of the combination $V(V+2)$ when the counterterm is expressed in terms of these fields. Furthermore, note that the counterterm only involves the pole-term $\frac{1}{\varepsilon}$ and γ_E , independent of any other parameters, for instance the mass parameter, in the $\overline{\text{MS}}$ renormalization scheme. We identify this counterterm (4.10) within the WKB result (4.6), with precisely the right coefficient and structure. We choose this particular $\overline{\text{MS}}$ renormalization prescription in order to compare with the work of Baacke and Lavrelashvili [22], who also use an $\overline{\text{MS}}$ prescription.

Combining Σ_1 and Σ_2 with the above renormalization counter term $\delta_{ct}S$, we get the one-loop effective action:

$$\begin{aligned} \Gamma_{\overline{\text{MS}}} = & \frac{1}{2} \ln |T_{(0)}(\infty)| - 2 \ln \left[\frac{\pi}{2} \Phi_\infty \left(\Phi_0 - \frac{3}{2} \Phi_0^2 + \frac{\alpha}{2} \Phi_0^3 \right) \right] \\ & + \frac{1}{2} \lim_{L \rightarrow \infty} \left\{ \sum_{l=2}^L (l+1)^2 \ln (T_{(l)}(\infty)) - \frac{(L+1)(L+2)}{4} \int_0^\infty dr r V(r) \right. \\ & \left. + \frac{\ln L}{8} \int_0^\infty dr r^3 V(V+2) \right\} - \frac{1}{16} \int_0^\infty dr \left(1 + \ln \frac{r}{2} \right) r^3 V(V+2) \end{aligned} \quad (4.11)$$

Here, the first two terms correspond to the $l = 0$ contribution (for the negative mode), computed using (3.12), and the $l = 1$ contribution (for the zero modes), computed using (3.13). The renormalized effective action $\Gamma_{\overline{\text{MS}}}$ is finite, and we obtain excellent convergence (accelerated by third order Richardson extrapolation [33]) for L of the order of 50 to 100, depending on the value of α . This result for $\Gamma_{\overline{\text{MS}}}$ is plotted in Figure 7 as a function of α .

We can alternatively express (4.11) with the L dependent WKB subtraction terms included as subtractions *inside* the l sum :

$$\begin{aligned} \Gamma_{\overline{\text{MS}}} = & \frac{1}{2} \ln |T_{(0)}(\infty)| - 2 \ln \left[\frac{\pi}{2} \Phi_\infty \left(\Phi_0 - \frac{3}{2} \Phi_0^2 + \frac{\alpha}{2} \Phi_0^3 \right) \right] \\ & + \frac{1}{2} \sum_{l=2}^\infty (l+1)^2 \left\{ \ln (T_{(l)}(\infty)) - \frac{\frac{1}{2} \int_0^\infty dr r V(r)}{(l+1)} + \frac{\frac{1}{8} \int_0^\infty dr r^3 V(V+2)}{(l+1)^3} \right\} \\ & - \frac{3}{4} \int_0^\infty dr r V(r) + \frac{1}{16} \int_0^\infty dr r^3 V(V+2) \left(\frac{1}{2} - \gamma_E - \ln \frac{r}{2} \right) \end{aligned} \quad (4.12)$$

Here we have simply used

$$\sum_{l=2}^L (l+1) = \frac{1}{2}(L+1)(L+2) - 3 \quad ; \quad \sum_{l=2}^L \frac{1}{(l+1)} \sim \ln L - \gamma_E \quad (4.13)$$

Thus, (4.12) shows that we can extend to next-to-leading order the large l behavior in (3.16)

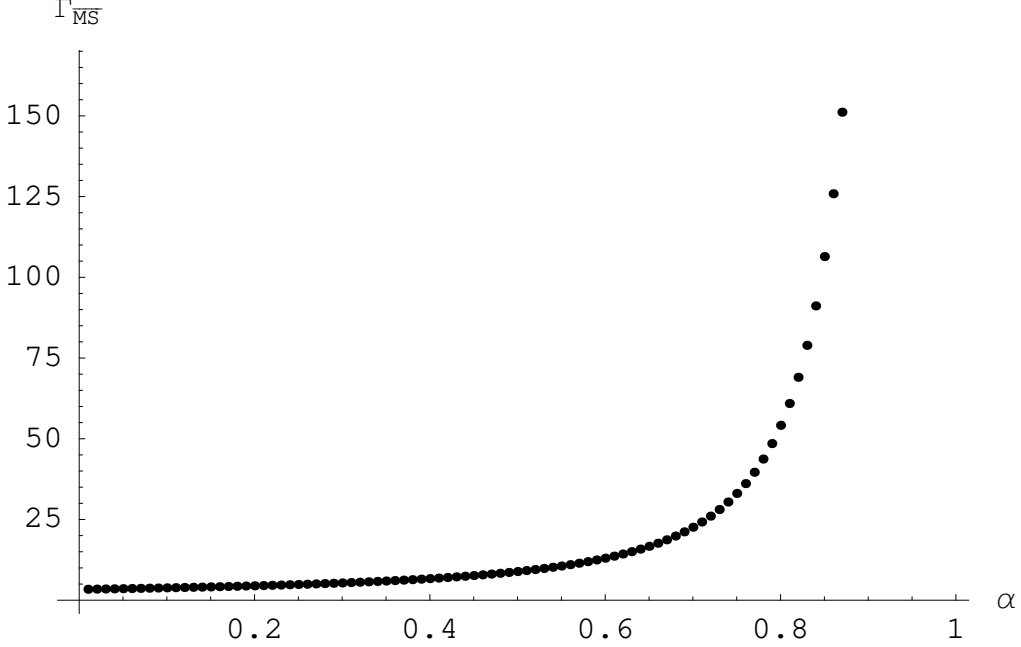


FIG. 7: Plot of the $\overline{\text{MS}}$ renormalized effective action (4.11) as a function of α .

of $\ln(T_{(l)}(\infty))$, the logarithm of the determinant of the radial operators in (3.1) :

$$\ln(T_{(l)}(\infty)) \sim \frac{\frac{1}{2} \int_0^\infty dr r V}{(l+1)} - \frac{\frac{1}{8} \int_0^\infty dr r^3 V(V+2)}{(l+1)^3} + O\left(\frac{1}{(l+1)^5}\right) \quad (4.14)$$

We have confirmed numerically that the remainder is indeed $O\left(\frac{1}{(l+1)^5}\right)$. Note that (4.14) provides a simple closed-form expression for the large l behavior of $\ln(T_{(l)}(\infty))$, and this expression is *local* in the fluctuation potential $V(r)$.

It is instructive to compare (4.12) with an expression obtained by Baacke and Lavreshavili [22] for the same quantity (note that the collective coordinate term, $-2 \ln\left(\frac{S_{\text{cl}}}{2\pi}\right)$, is separated out in [22]), also using the $\overline{\text{MS}}$ renormalization scheme :

$$\Gamma_{BL} = \frac{1}{2} \ln |T_{(0)}(\infty)| + 4 \frac{1}{2} \ln T'_{(1)}(\infty) + \frac{1}{2} \left(A_{\text{fin}}^{(1)} - \frac{1}{2} A_{\text{fin}}^{(2)} \right) + \frac{1}{2} \sum_{l=2}^{\infty} (l+1)^2 \left\{ \ln(T_{(l)}(\infty)) - h_l^{(1)}(\infty) - \left[h_l^{(2)}(\infty) - \frac{1}{2} \left(h_l^{(1)}(\infty) \right)^2 \right] \right\} \quad (4.15)$$

The second term corresponds to the fourfold degenerate zero modes, and is computed in [22] by evaluating the slope at zero with an additional parameter added to the operator in order to displace the determinant from zero. This agrees numerically with our expression in (3.13), [allowing for the collective coordinate term, $-2 \ln\left(\frac{S_{\text{cl}}}{2\pi}\right)$], but is more cumbersome

to evaluate. The subtractions $h_l^{(1)}(\infty)$ and $h_l^{(2)}(\infty)$ in (4.15) are associated with first and second order Feynman diagrams [22], and are given explicitly as the asymptotic values of $h_l^{(1)}(r)$ and $h_l^{(2)}(r)$, satisfying the differential equations

$$\begin{aligned} h_l^{(1)''} + \left(\frac{1}{r} + 2 \frac{I'_{l+1}(r)}{I_{l+1}(r)} \right) h_l^{(1)'} - V(r) &= 0 \\ h_l^{(2)''} + \left(\frac{1}{r} + 2 \frac{I'_{l+1}(r)}{I_{l+1}(r)} \right) h_l^{(2)'} - V(r) h_l^{(1)} &= 0 \quad , \end{aligned} \quad (4.16)$$

with *initial value boundary conditions*: $h_l(0) = 0$, and $h'_l(0) = 0$. The remaining terms in (4.15) are Born approximation terms

$$\begin{aligned} A_{\text{fin}}^{(1)} &= -\frac{1}{8} \int_0^\infty dr r^3 V(r) \\ A_{\text{fin}}^{(2)} &= \frac{1}{128\pi^4} \int_0^\infty dq q^3 |\tilde{V}(q)|^2 \left(2 - \sqrt{q^2 + 4} \ln \left[\frac{\sqrt{q^2 + 4} + q}{\sqrt{q^2 + 4} - q} \right] \right) \quad , \end{aligned} \quad (4.17)$$

where $\tilde{V}(q)$ is the Fourier transform of the fluctuation potential $V(r)$.

Note that Baacke and Lavrelashvili's expression (4.15) also gives a *finite* answer for the renormalized effective action. This means that we have another, quite different, expression for the large l behavior of $\ln(T_{(l)}(\infty))$:

$$\ln(T_{(l)}(\infty)) \sim h_l^{(1)}(\infty) + \left[h_l^{(2)}(\infty) - \frac{1}{2} \left(h_l^{(1)}(\infty) \right)^2 \right] + \dots \quad (4.18)$$

Comparing with (4.14), we deduce that the difference between these large l behaviors should agree to order $O\left(\frac{1}{(l+1)^4}\right)$. We have verified this numerically, and in fact we find that there is a nonzero difference at $O\left(\frac{1}{(l+1)^5}\right)$:

$$\begin{aligned} &\left\{ h_l^{(1)}(\infty) + \left[h_l^{(2)}(\infty) - \frac{1}{2} \left(h_l^{(1)}(\infty) \right)^2 \right] \right\} \\ &- \left\{ \frac{\frac{1}{2} \int_0^\infty dr r V(r)}{(l+1)} - \frac{\frac{1}{8} \int_0^\infty dr r^3 V(V+2)}{(l+1)^3} \right\} \sim O\left(\frac{1}{(l+1)^5}\right) \end{aligned} \quad (4.19)$$

Similarly, comparing the terms *outside* the l sums in (4.12) and (4.15), we see that these terms in (4.12) are *local* in the fluctuation potential $V(r)$, while $A_{\text{fin}}^{(2)}$ in (4.15) is *nonlocal* in $V(r)$. Nevertheless, the total quantities $\Gamma_{\overline{MS}}$ and Γ_{BL} are *equal* (allowing for the collective coordinate term, $-2 \ln\left(\frac{S_{\text{cl}}}{2\pi}\right)$, that is separated out in [22]), and we have confirmed this equality numerically. This means that (4.12) and (4.15) are different ways of regulating the l sum, and since each is renormalized using \overline{MS} , they should indeed be equal. In other

words, in (4.12) and (4.15), the different subtractions inside the l sums are compensated for by different finite pieces outside the l sums, in such a way that the total agrees. This is very similar to behavior found in the computation of mass shifts in soliton theories (see Appendix B of [34]). It is also a highly nontrivial check on both expressions. But, although the expressions (4.12) and (4.15) are equal, in purely pragmatic computational terms the local expression (4.12) is considerably simpler. First, the zero mode part is more easily and more accurately computed using (3.13), since it only requires the asymptotic properties of the (already computed) bounce solution $\Phi_{\text{cl}}(r)$. Second, one does not need to solve the differential equations (4.16) to find $h_l^{(1)}(\infty)$ and $h_l^{(2)}(\infty)$; instead, the large l behavior of $\ln T_{(l)}(\infty)$ is given by local expressions in $V(r)$. Third, one does not need to compute (numerically) the Fourier transform of the fluctuation potential, nor integrate the result over all momentum, as is necessary to compute A_2 in (4.17). Instead, all subtraction terms in (4.12) are purely *local* in the fluctuation potential $V(r)$.

In a series of papers studying the thin-wall approximation, Konoplich and Rubin [11, 15] have computed this same quantity with a related $\overline{\text{MS}}$ renormalization prescription, and obtained the following result in the $\alpha \rightarrow 1$ limit [we have translated their notation to match ours]:

$$\Gamma_{\text{KR}} \sim \frac{9}{32} \left[1 - \frac{2\pi}{9\sqrt{3}} \right] \frac{1}{(1-\alpha)^3} + O\left(\frac{1}{1-\alpha}\right) \quad . \quad (4.20)$$

Their renormalization prescription is such that this leading term can be compared directly to ours. The subleading terms in (4.20) are scheme dependent, except for a universal logarithmic term [11, 15]. The agreement with our result (4.12) is striking. Because of the divergence as $\alpha \rightarrow 1$, for plotting purposes it is useful to extract the overall factor of $\frac{1}{(1-\alpha)^3}$. In Figure 8 we plot our result (4.12), rescaled by a factor of $(1-\alpha)^3$, compared with the Konoplich-Rubin thin-wall approximation answer (4.20), also rescaled by a factor of $(1-\alpha)^3$. The intercept at $\alpha = 1$ is given by (4.20) to be

$$\frac{9}{32} \left[1 - \frac{2\pi}{9\sqrt{3}} \right] \approx 0.16788888 \quad , \quad (4.21)$$

which matches perfectly the $\alpha \rightarrow 1$ limit of our result (4.12), as can be clearly seen in Figure 8.

The $\overline{\text{MS}}$ prescription provides simple renormalization structures, but we can also use a “physical” renormalization prescription. For example, we may impose the following normal-

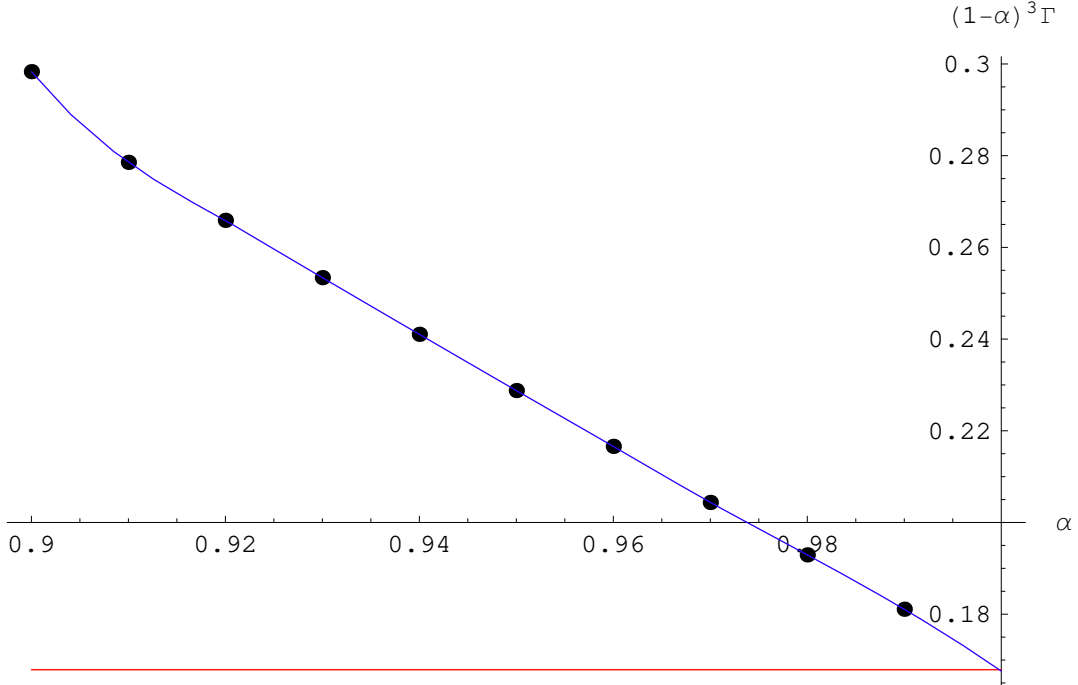


FIG. 8: Plot of the $\overline{\text{MS}}$ renormalized effective action, $\Gamma_{\overline{\text{MS}}}$, in (4.11), rescaled by a factor of $(1-\alpha)^3$, as a function of α in the thin-wall approximation limit as $\alpha \rightarrow 1$. The solid dots denote our data points for α in steps of 0.01 from 0.9 to 0.99, and the solid curve is an interpolation through these points. The horizontal line is the leading term of the Konoplich-Rubin result (4.20), also rescaled by a factor of $(1-\alpha)^3$. Note the excellent agreement at $\alpha = 1$.

ization condition to the one-loop effective potential,

$$\frac{d^2}{d\phi^2} (U_{\text{cl}} + U_{\text{eff}})|_{\phi=\phi_1} = \frac{\lambda}{2}(3\phi_1^2 - a^2), \quad \frac{d^4}{d\phi^4} (U_{\text{cl}} + U_{\text{eff}})|_{\phi=\phi_1} = 3\lambda. \quad (4.22)$$

In (4.22), $\phi_1 \equiv \phi_- + \delta\phi_-$ is the solution of the one-loop modified field equation

$$\frac{d}{d\phi} (U_{\text{cl}} + U_{\text{eff}})|_{\phi=\phi_1} = 0. \quad (4.23)$$

These normalization conditions can be satisfied when we change the renormalized parameters by finite amounts as $\lambda + \delta\lambda \rightarrow \lambda + \delta\lambda + \delta_{fin}\lambda$, and $\lambda a^2 + \delta(\lambda a^2) \rightarrow \lambda a^2 + \delta(\lambda a^2) + \delta_{fin}(\lambda a^2)$.

V. CONCLUSIONS

In conclusion, we have presented a simple and practical technique for evaluating the prefactor determinant in the expression for the metastable decay rate in scalar field theories.

The technique for computing the determinant is based on the Gelfand-Yaglom formula [19] for computing the determinant of a one-dimensional (here, radial) differential operator in terms of the asymptotic boundary value of an associated differential equation with initial value boundary conditions. This technique is extremely easy to implement for any given partial wave, but the naive sum over partial waves is divergent. Thus the direct application of the Gelfand-Yaglom formula to higher dimensions is not possible. However, this divergence can be regulated in various ways. Here we propose using the *angular momentum cutoff* regularization and renormalization scheme, which has been used previously to compute the explicit mass dependence of the fermion determinant in QCD for massive quarks in an instanton background [21]. In this approach the contribution of the low partial waves is computed numerically using the Gelfand-Yaglom formula, while the contribution of the high partial waves is computed analytically using radial WKB, which is a good approximation for large l . The merging of these two parts involves renormalization and we have illustrated our technique using an $\overline{\text{MS}}$ scheme in order to compare with the work of Baacke and Lavrelashvili [22], who also use the Gelfand-Yaglom technique, also with an $\overline{\text{MS}}$ prescription, but with a different regularization technique. We have shown that the two techniques agree, and have argued that the one presented here is somewhat easier to implement as it is purely *local* in the numerically determined fluctuation potential. The conversion to other renormalization schemes can be done using conventional field theory techniques, and corresponds to including finite polynomial terms in the effective potential. In an appendix we have derived a simple new formula for the $l = 1$ determinant with the zero modes removed, solely in terms of the asymptotic values of the bounce solution.

The goal of this work has been to reduce the computation of field theoretic one loop fluctuation determinants to a straightforward numerical exercise. As a by-product, we have found in (4.12) a simple extension of the Gelfand-Yaglom result to higher dimensional radially separable problems. There are many possible further applications of this technique, as there are many semiclassical problems where the classical solution, about which one is computing the quantum fluctuations, has radial symmetry. Closely related possible applications include: (i) metastable decay in theories with more than one field [36], where analytic and approximate approaches to the prefactor are quite difficult, but a direct numerical approach might be more useful; (ii) models in dimensions other than 4, which have been studied in and beyond the thin-wall approximation [6, 13, 14, 37]; (iii) an extension to finite temperature,

where the high temperature limit is essentially a dimensionally reduced 3d radial problem [9, 10], but for intermediate temperatures the explicit summation over Matsubara modes is necessary. This technique for computing precisely the fluctuation contribution may also be useful for a set of fascinating questions concerning the validity of Langer's homogeneous nucleation picture itself, as well as the semiclassical approximation [38]. More generally, our technique for extending the Gelfand-Yaglom formula to higher dimensions can also be applied to other symmetric semiclassical configurations such as vortices and monopoles (instantons were considered already in [21]).

Acknowledgments: We thank Holger Gies for helpful discussions. GD thanks the US DOE for support through the grant DE-FG02-92ER40716, and gratefully acknowledges the hospitality and support of Choonkyu Lee and the Center for Theoretical Physics at Seoul National University where part of this work was done.

VI. APPENDIX A : ZERO MODE CONTRIBUTION

In this Appendix we present a derivation of the expression (3.13) for the factor contributed by the $l = 1$ zero modes. We adapt a method of McKane and Tarlie [39] (see also [28, 29, 40]). First, add a small quantity, k^2 , to the operator possessing the zero mode, and to the corresponding free operator (although this latter addition is not important in the end). Then for small k^2 the existence of the four zero modes for \mathcal{M} [we suppress the ($l = 1$) subscript] implies that

$$\frac{\det(\mathcal{M} + k^2)}{\det(\mathcal{M}^{\text{free}} + k^2)} \sim (k^2)^4 \frac{\det' \mathcal{M}}{\det \mathcal{M}^{\text{free}}} \quad , \quad k^2 \rightarrow 0 \quad . \quad (6.1)$$

The result (3.4) means we can evaluate the LHS of (6.1) for arbitrary but small k^2 as

$$\frac{\det(\mathcal{M} + k^2)}{\det(\mathcal{M}^{\text{free}} + k^2)} = \left(\lim_{R \rightarrow \infty} \left(\frac{\psi_{k^2}(R)}{\psi_{k^2}^{\text{free}}(R)} \right) \right)^4 \quad , \quad (6.2)$$

where ψ_{k^2} satisfies

$$-\psi_{k^2}'' - \frac{3}{r}\psi_{k^2}' + \left(\frac{3}{r^2} + 1 + k^2 + V(r) \right) \psi_{k^2} = 0 \quad , \\ \psi_{k^2}(0) = 0 \quad ; \quad \psi_{k^2}'(0) = 1 \quad . \quad (6.3)$$

Note that for $l = 1$ we can express the $r \rightarrow 0$ boundary conditions (3.6) in this initial value form. The function $\psi_{k^2}^{\text{free}}$ satisfies the same equation and boundary conditions as in (6.3), but

with the potential V set to 0. So, one possible approach, as suggested in [22], to computing \det' is to compute the derivative of $\lim_{R \rightarrow \infty} \left(\frac{\psi_{k^2}(R)}{\psi_{k^2}^{\text{free}}(R)} \right)$ as $k^2 \rightarrow 0$. But a more direct and accurate method is as follows.

Define the function $\psi_0(r)$ to be the solution of (6.3) with $k^2 = 0$. Then by elementary integration by parts it follows that

$$\begin{aligned} 0 &= \int_0^R dr r^3 \psi_0 \left\{ -\frac{1}{r^3} (r^3 \psi'_{k^2})' + \left(\frac{3}{r^2} + 1 + k^2 + V(r) \right) \psi_{k^2} \right\} \\ &= [r^3 (\psi'_0 \psi_{k^2} - \psi_0 \psi'_{k^2})]_0^R + k^2 \int_0^R dr r^3 \psi_0 \psi_{k^2} \quad . \end{aligned} \quad (6.4)$$

Applying the boundary conditions at $r = 0$ we obtain

$$\psi_{k^2}(R) \left(1 - \frac{[\psi_0(R)]}{[\psi'_0(R)]} \frac{[\psi'_{k^2}(R)]}{[\psi_{k^2}(R)]} \right) = k^2 \frac{\int_0^R dr r^3 \psi_0 \psi_{k^2}}{(-R^3 \psi'_0(R))} \quad . \quad (6.5)$$

The important observation now is that $\psi_0(r)$ is actually the normalizable zero mode of \mathcal{M} , and decreases exponentially as e^{-r} at large r . On the other hand, for arbitrarily small but nonzero k^2 , the solution $\psi_{k^2}(r)$ *increases* exponentially as $e^{r\sqrt{1+k^2}}$ at large r . Thus at large R and arbitrarily small but nonzero k^2 , the identity (6.5) implies that the leading k^2 dependence at small k^2 is :

$$\psi_{k^2}(R) \sim \frac{1}{2} k^2 \frac{\int_0^R dr r^3 \psi_0^2}{(-R^3 \psi'_0(R))} \quad , \quad k^2 \rightarrow 0 \quad . \quad (6.6)$$

Then (6.2) leads to the following expression for the determinant with zero mode removed:

$$\frac{\det' \mathcal{M}}{\det \mathcal{M}^{\text{free}}} = \left(\frac{\int_0^\infty dr r^3 \psi_0^2}{\lim_{R \rightarrow \infty} [-2R^3 \psi'_0(R) \psi_0^{\text{free}}(R)]} \right)^4 \quad . \quad (6.7)$$

To simplify this general expression further, recall that the zero mode ψ_0 can be expressed in terms of the classical bounce solution :

$$\psi_0(r) = \frac{\Phi'_{\text{cl}}(r)}{\Phi''_{\text{cl}}(0)} \quad . \quad (6.8)$$

This has two important implications. First, the numerator on the RHS of (6.7) can be expressed in terms of the classical bounce action :

$$\begin{aligned} \int_0^\infty dr r^3 \psi_0^2 &= \frac{1}{2\pi^2 (\Phi''_{\text{cl}}(0))^2} \int d^4x (\bar{\Phi}'_{\text{cl}})^2 \\ &= \frac{1}{2\pi^2 (\Phi''_{\text{cl}}(0))^2} 4S_{\text{cl}}[\Phi_{\text{cl}}] \end{aligned} \quad (6.9)$$

Since $\frac{\det' \mathcal{M}}{\det \mathcal{M}^{\text{free}}}$ is raised to the power $-1/2$ on the LHS of (3.13), we see that the $S_{\text{cl}}[\Phi_{\text{cl}}]$ factors cancel. The second important implication of (6.8) is that the leading large R behavior of $\psi'_0(R)$ is determined by the coefficient Φ_∞ in (2.5). Since $\psi_0^{\text{free}}(r) = 8I_2(r)/r$, the denominator in (6.7) is

$$\begin{aligned} [-2R^3 \psi'_0(R) \psi_0^{\text{free}}(R)] &\sim -2R^3 \frac{\Phi_\infty}{\Phi_{\text{cl}}''(0)} \left(\frac{K_1(r)}{r} \right)'' \Big|_{r=R} \left(\frac{8I_2(R)}{R} \right) \\ &\rightarrow -8 \frac{\Phi_\infty}{\Phi_{\text{cl}}''(0)} \quad , \quad R \rightarrow \infty \quad . \end{aligned} \quad (6.10)$$

Thus we obtain the simple formula

$$\left(\frac{S_{\text{cl}}[\Phi_{\text{cl}}]}{2\pi} \right)^2 \left(\frac{\det' \mathcal{M}_{(l=1)}}{\det \mathcal{M}_{(l=1)}^{\text{free}}} \right)^{-1/2} = [2\pi \Phi_\infty \Phi_{\text{cl}}''(0)]^2 . \quad (6.11)$$

The final result (3.13) follows by noting that $\Phi_{\text{cl}}''(0)$ may be expressed in terms of $\Phi_{\text{cl}}(0)$ using the bounce differential equation (2.1) and the boundary condition (2.2).

We stress that the final expression (3.13) only requires knowing the two asymptotic constants, Φ_∞ and $\Phi_{\text{cl}}(0)$, each of which is determined to great precision in the course of finding the classical bounce solution numerically, as described in Section III.

-
- [1] J. S. Langer, “Theory Of The Condensation Point,” *Annals Phys.* **41**, 108 (1967); “Statistical Theory Of The Decay Of Metastable States,” *Annals Phys.* **54**, 258 (1969).
- [2] M. B. Voloshin, I. Y. Kobzarev, and L. B. Okun, “Bubbles In Metastable Vacuum,” *Sov. J. Nucl. Phys.* **20**, 644 (1975) [*Yad. Fiz.* **20**, 1229 (1974)].
- [3] M. Stone, “The Lifetime And Decay Of ‘Excited Vacuum’ States Of A Field Theory Associated With Nonabsolute Minima Of Its Effective Potential,” *Phys. Rev. D* **14**, 3568 (1976); “Semiclassical Methods For Unstable States,” *Phys. Lett. B* **67**, 186 (1977); *The Physics of Quantum Fields*, Springer (New York, 2000).
- [4] S. R. Coleman, “The Fate Of The False Vacuum. 1. Semiclassical Theory,” *Phys. Rev. D* **15**, 2929 (1977) [Erratum-ibid. *D* **16**, 1248 (1977)]; C. G. Callan and S. R. Coleman, “The Fate Of The False Vacuum. 2. First Quantum Corrections,” *Phys. Rev. D* **16**, 1762 (1977); S. R. Coleman, “The Uses Of Instantons,” *Lectures delivered at 1977 International School of Subnuclear Physics, Erice: The Whys of subnuclear physics*, Edited by A. Zichichi, (Plenum Press, 1979).

- [5] I. K. Affleck and F. De Luccia, “Induced Vacuum Decay,” *Phys. Rev. D* **20**, 3168 (1979).
- [6] M. B. Voloshin, “Decay Of a Metastable Vacuum In (1+1)-Dimensions,” *Yad. Fiz.* **42**, 1017 (1985), [*Sov. J. Nucl. Phys.* **42**, 644 (1985)].
- [7] E. Weinberg, “Vacuum Decay in theories with symmetry breaking by radiative corrections,” *Phys. Rev. D* **47**, 4614 (1993).
- [8] M. B. Voloshin, “False vacuum decay,” *Lectures given at International School of Subnuclear Physics: 33rd Course: Vacuum and Vacua: the Physics of Nothing, Erice, 1995*, Edited by A. Zichichi, (World Scientific, Singapore, 1996).
- [9] A. D. Linde, “Fate Of The False Vacuum At Finite Temperature: Theory And Applications,” *Phys. Lett. B* **100**, 37 (1981); “Decay Of The False Vacuum At Finite Temperature,” *Nucl. Phys. B* **216**, 421 (1983) [Erratum-ibid. *B* **223**, 544 (1983)].
- [10] I. Affleck, “Quantum Statistical Metastability,” *Phys. Rev. Lett.* **46**, 388 (1981).
- [11] R. V. Konoplich, “On Probability Of Decay Of Metastable Vacuum),” *Yad. Fiz.* **32**, 1132 (1980); R. V. Konoplich and S. G. Rubin, “Quantum Corrections To Nontrivial Classical Solutions In Φ^4 Theory,” *Yad. Fiz.* **37**, 1330 (1983).
- [12] V. G. Kiselev and K. G. Selivanov, “Calculation Of The Functional Determinant In The Vacuum Explosion Problem,” *JETP Lett.* **39**, 85 (1984) [*Pisma Zh. Eksp. Teor. Fiz.* **39**, 72 (1984)]; “Metastable Vacuum Decay In Two-Dimensional Field Theory,” *Sov. J. Nucl. Phys.* **43**, 153 (1986) [*Yad. Fiz.* **43**, 239 (1986)].
- [13] G. Munster and S. Rotsch, “Analytical calculation of the nucleation rate for first order phase transitions beyond the thin wall approximation,” *Eur. Phys. J. C* **12**, 161 (2000) [arXiv:cond-mat/9908246]; G. Munster and S. B. Rutkevich, “Semiclassical calculation of the nucleation rate for first order phase transitions in the 2-dimensional ϕ^4 -model beyond the thin wall approximation,” arXiv:cond-mat/0009016; G. Munster and S. B. Rutkevich, “The classical nucleation rate in two dimensions,” *Eur. Phys. J. C* **27**, 297 (2003).
- [14] M. B. Voloshin, “The rate of metastable vacuum decay in (2+1) dimensions,” *Phys. Lett. B* **599**, 129 (2004) [arXiv:hep-th/0407061].
- [15] R. V. Konoplich and S. G. Rubin, “Decay Probability For Metastable Vacuum In Scalar Theory,” *Yad. Fiz.* **42**, 1282 (1985), [*Sov. J. Nucl. Phys.* **42**, 810 (1986)]; “Decay of the Metastable Vacuum,” *Yad. Fiz.* **44**, 558 (1986), [*Sov. J. Nucl. Phys.* **44**, 359 (1986)]; R. V. Konoplich, “Calculation Of Quantum Corrections To Nontrivial Classical Solutions By Means Of The

- Zeta Function,” *Theor. Math. Phys.* **73**, 1286 (1987) [*Teor. Mat. Fiz.* **73**, 379 (1987)].
- [16] M. G. Alford, H. Feldman and M. Gleiser, “Thermal activation of metastable decay: Testing nucleation theory,” *Phys. Rev. D* **47**, 2168 (1993); M. G. Alford and M. Gleiser, “Metastability in two-dimensions and the effective potential,” *Phys. Rev. D* **48**, 2838 (1993) [arXiv:hep-ph/9304245].
- [17] A. Strumia and N. Tetradis, “A consistent calculation of bubble-nucleation rates,” *Nucl. Phys. B* **542**, 719 (1999) [arXiv:hep-ph/9806453]; “Testing nucleation theory in two dimensions,” *Nucl. Phys. B* **560**, 482 (1999) [arXiv:hep-ph/9904246].
- [18] I. G. Moss and W. Naylor, “Effective action for bubble nucleation rates,” *Nucl. Phys. B* **632**, 173 (2002) [arXiv:hep-ph/0102104].
- [19] I. M. Gelfand and A. M. Yaglom, “Integration In Functional Spaces And It Applications In Quantum Physics,” *J. Math. Phys.* **1**, 48 (1960).
- [20] R. Forman, “Functional determinants and geometry”, *Invent. Math.* **88**, 447 (1987); Erratum, *ibid* **108**, 453 (1992).
- [21] G. V. Dunne, J. Hur, C. Lee and H. Min, “Precise quark mass dependence of instanton determinant,” *Phys. Rev. Lett.* **94**, 072001 (2005) [arXiv:hep-th/0410190]; “Calculation of QCD instanton determinant with arbitrary mass,” *Phys. Rev. D* **71**, 085019 (2005) [arXiv:hep-th/0502087].
- [22] J. Baacke and G. Lavrelashvili, “One-loop corrections to the metastable vacuum decay,” *Phys. Rev. D* **69**, 025009 (2004) [arXiv:hep-th/0307202].
- [23] S. R. Coleman and E. Weinberg, “Radiative Corrections As The Origin Of Spontaneous Symmetry Breaking,” *Phys. Rev. D* **7**, 1888 (1973).
- [24] A. Salam and J. A. Strathdee, “Comment On The Computation Of Effective Potentials,” *Phys. Rev. D* **9**, 1129 (1974); R. Jackiw, “Functional Evaluation Of The Effective Potential,” *Phys. Rev. D* **9**, 1686 (1974); J. Iliopoulos, C. Itzykson and A. Martin, “Functional Methods And Perturbation Theory,” *Rev. Mod. Phys.* **47**, 165 (1975).
- [25] S. R. Coleman, V. Glaser and A. Martin, “Action Minima Among Solutions To A Class Of Euclidean Scalar Field Equations,” *Commun. Math. Phys.* **58**, 211 (1978).
- [26] S. Levit and U. Smilansky, “A theorem on infinite products of eigenvalues of Sturm-Liouville type operators”, *Proc. Am. Math. Soc.* **65**, 299 (1977).
- [27] S. R. Coleman, “The Uses Of Instantons,” *Lecture delivered at 1977 Int. School of Subnuclear*

Physics, Erice, Italy, Jul 23-Aug 10, 1977.

- [28] K. Kirsten, *Spectral Functions in Mathematics and Physics*, (Chapman-Hall, Boca Raton, 2002).
- [29] K. Kirsten and A. J. McKane, “Functional determinants by contour integration methods,” *Annals Phys.* **308**, 502 (2003) [arXiv:math-ph/0305010]; “Functional determinants for general Sturm-Liouville problems,” *J. Phys. A* **37**, 4649 (2004) [arXiv:math-ph/0403050].
- [30] H. Kleinert, “Path Integrals in Quantum Mechanics, Statistics, Polymer Physics, and Financial Markets,” (World Scientific, Singapore, 2004).
- [31] J. L. Gervais and B. Sakita, “Wkb Wave Function For Systems With Many Degrees Of Freedom: A Unified View Of Solitons And Pseudoparticles,” *Phys. Rev. D* **16**, 3507 (1977).
- [32] G. V. Dunne, J. Hur, C. Lee and H. Min, “Instanton determinant with arbitrary quark mass: WKB phase-shift method and derivative expansion,” *Phys. Lett. B* **600**, 302 (2004) [arXiv:hep-th/0407222].
- [33] C. M. Bender and S. A. Orszag, *Advanced Mathematical Methods for Scientists and Engineers*, (McGraw-Hill Inc., New York, 1978).
- [34] E. Farhi, N. Graham, R. L. Jaffe and H. Weigel, “Searching for quantum solitons in a 3+1 dimensional chiral Yukawa model,” *Nucl. Phys. B* **630**, 241 (2002) [arXiv:hep-th/0112217].
- [35] M. E. Peskin and D. V. Schroeder, *An Introduction to quantum field theory*, (Addison-Wesley, Reading, 1995).
- [36] E. J. Weinberg, “Vacuum decay in theories with symmetry breaking by radiative corrections,” *Phys. Rev. D* **47**, 4614 (1993) [arXiv:hep-ph/9211314]; A. Kusenko, “Improved action method for analyzing tunneling in quantum field theory,” *Phys. Lett. B* **358**, 51 (1995) [arXiv:hep-ph/9504418]; A. Kusenko, P. Langacker and G. Segre, “Phase Transitions and Vacuum Tunneling Into Charge and Color Breaking Minima in the MSSM,” *Phys. Rev. D* **54**, 5824 (1996) [arXiv:hep-ph/9602414]; A. Kusenko, Kimyeong Lee and E. J. Weinberg, “Vacuum decay and internal symmetries,” *Phys. Rev. D* **55**, 4903 (1997) [arXiv:hep-th/9609100].
- [37] N. J. Guenther, D. A. Nicole and D. J. Wallace, “Goldstone Modes In Vacuum Decay And First Order Phase Transitions,” *J. Phys. A* **13**, 1755 (1980).
- [38] A. Strumia, N. Tetradis and C. Wetterich, “The region of validity of homogeneous nucleation theory,” *Phys. Lett. B* **467**, 279 (1999) [arXiv:hep-ph/9808263]; G. Munster, A. Strumia and N. Tetradis, “Comparison of two methods for calculating nucleation rates,” *Phys. Lett. A*

- 271**, 80 (2000) [arXiv:cond-mat/0002278].
- [39] A. J. McKane and M. B. Tarlie, “Regularisation of functional determinants using boundary perturbations,” *J. Phys. A* **28**, 6931 (1995) [arXiv:cond-mat/9509126].
- [40] H. Kleinert and A. Chervyakov, “Simple Explicit Formulas for Gaussian Path Integrals with Time-Dependent Frequencies,” *Phys. Lett. A* **245**, 345 (1998) [arXiv:quant-ph/9803016].